DIFFERENTIAL SAR INTERFEROMETRY FOR LAND SUBSIDENCE MONITORING: METHODOLOGY AND EXAMPLES

Urs Wegmüller and Tazio Strozzi

Gamma Remote Sensing, Thunstrasse 130, 3074 Muri BE, Switzerland

Luigi Tosi

Istituto per lo Studio della Dinamica delle Grandi Masse, CNR, 30125 Venezia, Italy

Abstract

In recent years significant progress was achieved in SAR interferometry. In this paper we report on the potential of differential SAR interferometry to map land subsidence. After a presentation of the methodology the focus will be on feasibility demonstration and accuracy assessment. The theoretical considerations are verified with the selected cases Ruhrgebiet, Mexico City, Bologna, and Euganean Geothermal Basin, representing fast (*m/year*) to slow (*mm/year*) deformation velocities.

The accuracy of the generated deformation maps, the huge SAR data archive starting in 1991, the expected continued availability of new data, and the maturity of the required processing techniques, lead to the conclusion that differential SAR interferometry has a very high potential for operational mapping of land subsidence.

Keywords: subsidence, SAR interferometry, interferogram stacking, accuracy assessment.

1. Introduction

The potential of differential Synthetic Aperture Radar (SAR) interferometry to map coherent displacement at c*m* to *mm* resolution resulted in spectacular new results for geophysical sciences. Earthquake displacement (Massonnet et al., 1993), volcano deformation (Massonnet et al., 1995), glacier dynamics (Goldstein et al., 1993), and land subsidence (Strozzi et al., 1999a, 1999b, Wegmüller et al., 1999) were mapped. The required data are provided by the space-borne SAR sensors on the ERS-1, ERS-2, Radarsat, and JERS satellites. The planned follow-on sensors on ENVISAT and ALOS will guarantee the availability of appropriate data into the future.

The objectives of this contribution are the presentation of the SAR interferometric methodology and the assessment of its performance. A special focus will be on the interferogram stacking technique, a combination of multiple interferograms which allows to reduce the error introduced by atmospheric distortions, the main error source in SAR interferometry.

2. Differential SAR interferometry

Until recently, the phase in SAR imagery was not considered since it is uniformly distributed in the interval [-π,π] for rough surfaces. However, two images acquired from almost the identical aspect angle have almost the same identical speckle. Under such conditions the phase difference ϕ is related to the imaging path length difference

$$\phi = -\frac{4\pi}{\lambda}(|\boldsymbol{r_2}| - |\boldsymbol{r_1}|), \tag{1}$$

where λ is the radar signal wavelength. The phase is determined as the argument of the normalized interferogram, γ, defined as the normalized complex correlation coefficient of the complex backscatter intensities s_1 and s_2 at positions $\boldsymbol{r_1}$ and $\boldsymbol{r_2}$

$$\gamma = \frac{\langle s_2 s_1^* \rangle}{\sqrt{\langle s_1 s_1^* \rangle \langle s_2 s_2^* \rangle}}, \tag{2}$$

with the brackets $\langle x \rangle$ standing for the ensemble average of x. The variance of the estimate of the interferometric phase $\hat{\phi}$ is reduced by coherent averaging over statistically independent samples. The degree of coherence, a measure of the phase noise, is defined as the magnitude of the normalized interferogram $\gamma = |\gamma|$.

The interferometric imaging geometry formed by two passes of a radar sensor separated by the baseline *B* is shown in Fig. 1. The interferometric phase is sensitive to both surface topography and coherent displacement along the look vector occurring between the acquisition of the interferometric image pair. Inhomogeneous propagation delay and phase noise are the main error sources. The unwrapped interferometric phase ϕ_{unw} can be expressed as a sum of a topographic term ϕ_{topo}, a displacement term ϕ_{disp}, a path delay term ϕ_{path}, and a phase noise (or decorrelation) term ϕ_{noise}:

$$\phi_{unw} = \phi_{topo} + \phi_{disp} + \phi_{path} + \phi_{noise}. \tag{3}$$

The phase to height sensitivity,

$$\delta\phi_{topo} = \frac{4\pi}{\lambda}\frac{B_\perp}{r \cdot \cos\theta}\delta h, \tag{4}$$

with the wavelength, λ, the baseline component perpendicular to the look vector, $B_\perp$, the incidence angle, θ, and the slant range, r, characterizes the topographic term. Knowing the baseline geometry and ϕ_{topo} allows to calculated the exact look angle and together with the orbit information the position of the scatter elements allowing to derive the surface topography.

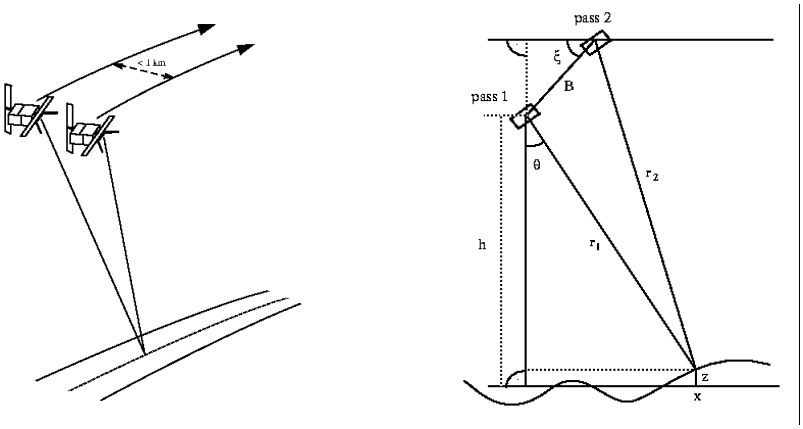

Fig. 1: Interferometric imaging geometry showing the two passes with range vectors $\boldsymbol{r_1}$ and $\boldsymbol{r_2}$ to the resolution element. The look angle of the radar is θ. The baseline B is tilted at an angle ξ measured relative to horizontal.

The displacement term, ϕ_{disp}, is related to the *coherent* displacement of the scattering centers along the radar look vector, r_{disp}:

$$\phi_{disp} = 2kr_{disp}, \tag{5}$$

where k is the wavenumber. In this context *coherent* means that the same displacement is observed for adjacent scatter elements. Under the assumption of exclusively vertical displacement Equation 5 can be converted to

$$\phi_{disp} = \frac{2kr_{sub}}{cos\theta}, \tag{6}$$

where r_{sub} is the vertical displacement. The sensitivity of ϕ_{disp} to surface deformation is very high. In the case of ERS, for example, 2π displacement phase corresponds to only 2.7 *cm* displacement along the look vector or 3 *cm* of vertical subsidence. Vertical subsidence can usually be assumed in the case of ground water extraction. In the case of mining induced subsidence, on the other hand, the observed geometry of the ground movement is more complicated. Even a combination of SAR data acquired in ascending and descending mode does not allow to resolve the complete three dimensional displacement vector field, without use of additional information.

The path delay term ϕ_{path} is the result of spatial inhomogeneity in the atmospheric conditions (mainly water vapor content). *(see Section 3)*

The decorrelation term ϕ_{noise} is caused by random (or incoherent) displacement of the scattering centers and by SAR signal noise. Multi-looking and filtering of the interferogram allow to reduce the phase noise. The main difficulty with high phase noise is not so much the statistical error introduced in the estimation of ϕ_{topo} and ϕ_{disp} but resulting phase unwrapping problems. Ideally, the phase noise and the phase difference between adjacent pixels are both much smaller than π. In reality this is often not the case, especially for areas with a low coherence and rugged topography. The coherence of ERS

Tandem pairs (1 day acquisition time interval) is very low for open water and forest and higher for most other classes. For a 35 day time interval the coherence is still quite high over sparsely vegetated terrain. For acquisition intervals longer than one year the areas with higher coherence levels are further reduced mainly to urban and sub-urban areas.

The basic idea of the differential interferometric approach is to separate the effects of surface topography and coherent displacement, allowing to retrieve differential displacement maps *(Wegmüller and Strozzi, 1998a, Wegmüller and Strozzi, 1998b)*. This goal is achieved by subtracting the topography related phase, ϕ_{topo}, which is either calculated based on a available Digital Elevation Model (DEM) or estimated from an independent interferogram with a short acquisition interval, such as an ERS Tandem pair. In many cases the use of a DEM turns out to be more robust and operational. The phase unwrapping required in the multi-pass approach is often difficult to resolve and far from operational for low coherence areas, especially in rugged terrain. In addition, gaps in the unwrapped topographic phase for areas of too low coherence may be present, depending on the phase unwrapping method used. Because of the scaling of the topographic phase with the perpendicular baseline component (Equation 4) the accuracy of baseline estimation is very important. At present we use various estimation methods based on the orbits data, the registration offsets, and the fringe rate of the interferogram. The error in a displacement measurement resulting from inaccurate baseline increases with the size of the area investigated.

Data processing related aspects which influence the robustness and operationality of the application as well as the accuracy of the result include phase filtering, phase unwrapping, geocoding, and the averaging scheme for multiple results. More details on the processing chain used for the generation of the results presented in this paper are found in Wegmüller and Strozzi, 1998b.

3. Accuracy considerations and interferogram stacking technique

The path delay term ϕ_{path} of Equation 3 is the result of spatial heterogeneity of the atmospheric (mainly water vapor content) and ionospheric conditions. These so-called *'atmospheric distortions'* are the main error source of SAR interferometry. As a relatively strong atmospheric distortion we consider a phase error of $\pi/2$. This relatively high error value is not just motivated by a rather conservative assessment of the accuracy, but also to achieve a more robust and operational technique. High atmospheric errors can often be identified by its specific shape, by cross-comparison of multiple interferograms, or possibly based on meteorological data. It is not clear, though, how to best integrate such tests in an operational processing chain.

For the ERS SAR configuration an atmospheric distortion of $\pi/2$ results in an error of approximately 0.75 *cm* in the estimation of a vertical displacement. To obtain reliable displacement values with SAR interferometry the subsidence

signal should dominate over the error terms. To keep the expected error in the order of 5% of the maximum displacement the displacement phase term should be 20 times the assumed atmospheric distortion, i.e. 10π, or about 15 *cm* of vertical subsidence. With this in mind, we preferably select an interferogram with 3 or more years acquisition interval to map a subsidence velocity of 5 *cm/year*. To map higher subsidence velocities shorter intervals are preferred, allowing a better temporal resolution of the subsidence history. In addition, the coherence is higher for shorter time intervals allowing a more complete spatial coverage. To map slow subsidence, longer intervals are required. The intervals cannot be freely extended because of the limited mission duration. In addition, the use of very long intervals introduces excessive temporal decorrelation, which precludes interpretation of data except for urban areas. Furthermore, the temporal resolution of the monitoring is reduced.

An approach to improve the ratio between the subsidence signal and the atmospheric phase error is the stacking of multiple interferograms. Under the assumption of a stationary process the subsidence term adds up linearly, i.e. the addition of the unwrapped phases of two interferograms with one and two years acquisition intervals results in an unwrapped phase covering an effective time interval of 3 years. For the error term, on the other hand, we can assume statistical independence between independent interferograms resulting in an increase with the square root of the number of pairs. The relative subsidence velocity estimation error is calculated as

$$\frac{\Delta r_{sub}}{r_{sub}} = \frac{\sqrt{n} \cdot E}{v \cdot \sum t_i}. \tag{7}$$

with n the number of independent interferograms used, E the absolute error estimate for a single interferogram, v the subsidence velocity, and $\sum t_i$ the cumulative time interval. Equation 7 can be used to determine the cumulative time required to map a certain subsidence velocity with a predefined expected relative estimation error (see Figure 2 for ERS SAR data). The potential of the interferogram stacking technique is demonstrated by the fact that the stacking of more than 10 independent interferograms allowing to reach a cumulative time interval of more than 20 years results in an expected subsidence velocity estimation error below 1 *mm/year*. Such stacking is indeed possible thanks to the immense ERS data archive. The condition, that the estimation accuracy can be expected to improve if an additional interferogram is added to a stack of n interferograms,

$$\frac{t_{n+1}}{\sum_n t_i} \geq \frac{\sqrt{n+1}}{\sqrt{n}} - 1, \tag{8}$$

depends only on the relative increase of the cumulative time and the number of independent interferograms in the stack.

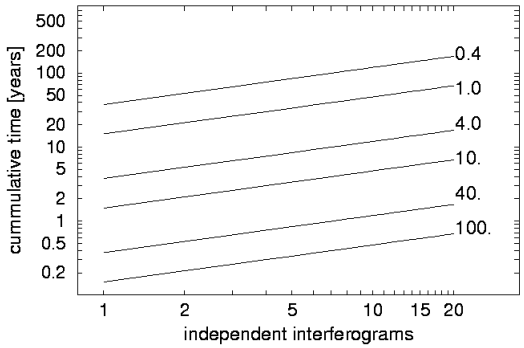

Figure 2: Quality assurance plot used in ERS data selection for interferogram stacking as calculated for an atmospheric distortion of $\pi/2$. For the selected subsidence velocities, 0.4 *cm/year*, 1.0 *cm/year*, 4.0 *cm/year*, 10.0 *cm/year*, 40.0 *cm/year*, and 100 *cm/year* the lines indicate the cumulative time required to achieve with the indicated number of independent interferograms a relative estimation error of 5%.

4. Examples

Four sites characterized by different displacement velocities were selected to investigate the performance of differential SAR interferometry for land subsidence monitoring: the Ruhrgebiet (Germany), Mexico City (Mexico), Bologna (Italy), and the Euganean Geothermal Basin (Italy). In the case of Bologna the subsidence was first estimated using single interferograms with acquisition time intervals of more than three years. In a second phase the feasibility of an annual subsidence monitoring was investigated using the interferogram stacking technique. The approximate subsidence velocities, the monitoring interval selected, the number of interferograms used and the expected estimation error are summarized in Table 1. In the following the results achieved for the four sites will be summarized.

Table 1: Subsidence velocities for the selected sites. In all cases SAR data of the European Remote Sensing Satellites ERS-1 and ERS-2 were used.

	Velocities *[cm/year]*	Monitoring interval	Interferograms / Cumulative time	Expected accuracy[1] *[cm/year]*
Ruhrgebiet (Germany)	0 - 200	1 month	1 / 1 month	9.0
Mexico City (Mexico)	0 - 40	3 months	1 / 3 months	3.0
Bologna (Italy)	0 - 4	4 years	3 / 9 years	0.15
Bologna (Italy)	0 - 4	1 year	6 / 4 years	0.5
Euganean Geothermal Basin (Italy)	0 - 0.4	5 years	10 / 20 years	0.1

[1] as calculated for an atmospheric distortion of $\pi/2$. No other errors considered.

4.1 Ruhrgebiet

Coal mining causes significant surface movement in the German Ruhrgebiet. Due to legal requirements the mining companies are obliged to assess the environmental impact of the excavations. Surface deformation caused by mining is a very dynamic process with high spatial and temporal variability. For mining areas with high subsidence velocities, interferometric pairs with acquisition intervals of only one or a few 35 day repeat cycles are preferred. Subsidence maps of different time intervals clearly indicate the progress in the sub-surface coal excavation. Figure 3 shows an example of a typical deformation cone observed for areas of active excavation. The colors indicate the deformation along the SAR observation direction. One color cycle corresponds to a displacement of 2.7 *cm* during the 35 days time interval. Vertical subsidence cannot be assumed in this case of mining induced deformation. The white color indicates areas of low coherence where the phase could not be unwrapped. Detailed studies and a validation with excavation plans are ongoing.

4.2 Mexico City

Mexico City is built on highly compressible clays and by reason of strong groundwater extraction a total subsidence of more than nine meters has been observed over the last century. The selection of ERS data to map subsidence at Mexico City is strongly restricted by the relatively few acquisitions found in the archive. From the available data acquisitions, three independent differential interferograms, one in ascending and two in descending mode, were selected. The subsidence maps derived from the three independent interferograms are consistent. For the period January 1996 – May 1996 (Figure 4) the observed maximum subsidence velocities are about 40cm/year, in general agreement with those reported in the literature and derived form levelling surveys and theoretical models. For a more detailed description of this case see Strozzi and Wegmüller, 1999a.

4.3 Bologna

At Bologna, Italy, the subsiding area is large with maximum subsidence velocities of 6 to 8 *cm/year* and characteristic spatial gradients of the vertical movement. Levelling surveys are being conducted at intervals of several years. We decided to use this case to investigate the potential of differential SAR interferometry because of the large science community involved in this case and the available reference data which can be used for validation purposes. A more detailed discussion of the interferometric investigation is given by Strozzi et al. (2000). Here, the focus is on the evaluation of the performance of the technique.

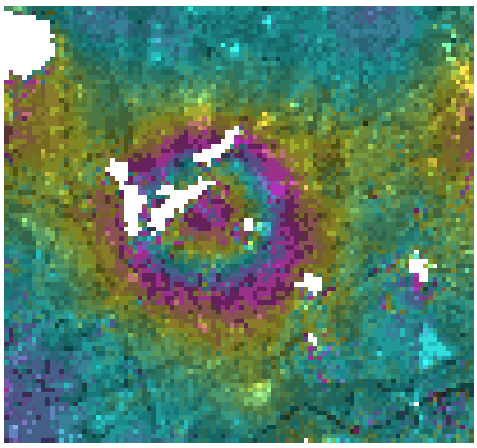

Figure 3. Ruhrgebiet: deformation map for active coal excavation site. The image width is 2.5 *km*. The color scale is defined in the text. For the image brightness the backscattering coefficient is used.

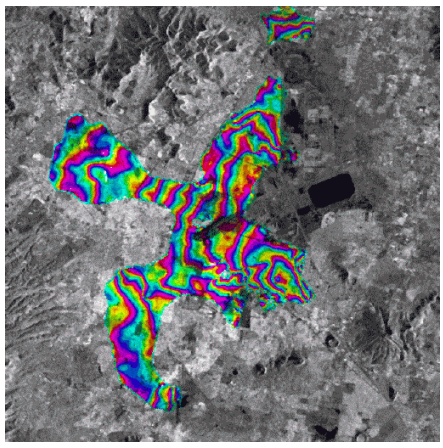

Fig. 4. Mexico City: interferometric subsidence map derived from the ERS pair 29-Dec-1995 / 16-May-1996. Subsidence velocity per color cycle: 5 *cm/year*. For the image brightness the backscattering coefficient is used.

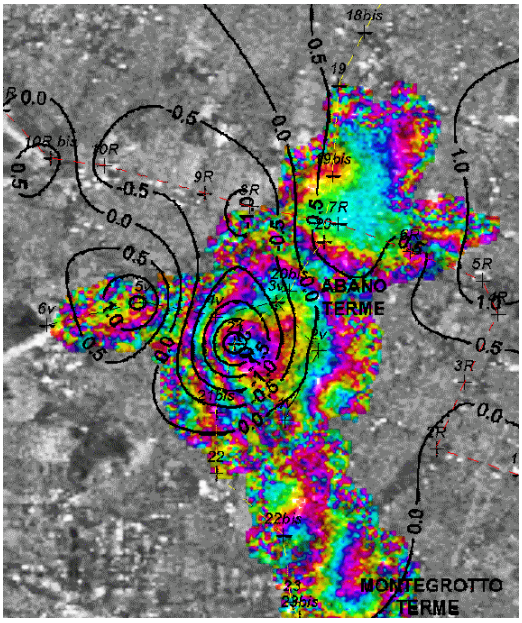

Figure 5. Vertical ground movements (in *mm/year)* from levelling surveys in 1991 and 1995 in the urban areas of Abano and Montegrotto Terme (data from Comune di Abano Terme and Regione del Veneto) superposed to the interferometric displacement velocity map for the interval 1992 to 1996. Also shown are the position of the levelling lines and benchmarks.

In a first step three long-time ERS interferometric pairs were selected (Wegmüller at al., 1999). Cross-comparison of the three resulting subsidence maps was used as an immediate quality check, confirming good consistency between the results. In a next step interferogram stacking was applied. The resulting interferometry based subsidence map was then validated with levelling data. For the urban area of Bologna the absolute values and the shapes of the contour lines of the interferometric subsidence map are in good agreement with those derived from levelling surveys. The quantitative validation, nevertheless, indicated a systematic offset between the subsidence velocity values determined from levelling surveys (period 1987-1992) and SAR interferometry (period 1992-1996). This difference can be explained by the different observation time period, indicating a decrease of the subsidence velocity. To confirm this interpretation more recent levelling data with a better correspondence to the time interval covered with SAR interferometry will be used for the validation as soon as such data will become available.

The hypothesis of the temporal decrease of the subsidence velocity at Bologna raised our interest in a better temporal resolution of the subsidence monitoring. To investigate the feasibility of an annual monitoring with differential SAR interferometry we produced subsidence maps for the time periods 1992-1993 and 1997-1998 applying the interferogram stacking technique with 6 and 7 interferograms, respectively, and cumulative time intervals of more than four years. The comparison of the two subsidence maps confirmed the decrease of the subsidence activity in Bologna during the last decade. The 1992-1993 map was validated with the 1987-1992 levelling surveys (Strozzi et al., 2000), confirming the expected feasibility of an annual subsidence monitoring. Up to present the 1997-1998 result could not be validated.

4.4 Euganean Geothermal Basin

Land subsidence of the Euganean Geothermal Basin, Italy, is related to the geothermal groundwater withdrawal. Precision levelling surveys conducted for the Commune di Abano Terme and the Regione del Veneto indicate maximum subsidence rates of 1 *cm/year* for the period up to 1991. After 1991 the subsidence velocity decreased as a consequence of a regulation of the groundwater withdrawal. In our investigation this case is used to analyze the feasibility of differential interferometric monitoring of slow subsidence velocities.

To map the expected low sub-*cm/year* subsidence velocity 10 interferograms in the time span 1992 to 1996 were selected. Interferogram stacking was used to generate a single subsidence map with a cumulative time interval of more than 20 years, allowing to reduce the expected velocity estimation error caused by atmospheric phase distortions to approximately 1 *mm/year*, a level which is significantly below the expected subsidence level of several *mm/year*.

The resulting interferometric deformation map shows a clear subsidence over Abano Terme with a maximum velocity of 4 *mm/year*, in agreement with the results of the last levelling surveys performed in 1991 and 1995 (Figure 5). The correspondence of the results of the two different surveying techniques is high, as confirmed by a direct quantitative validation of the interferometry based subsidence values along the levelling lines, an example of which is shown in Figure 6. For 17 points where we had values available from both surveying techniques the average difference of the vertical displacement velocity values was 0.2 mm/year with a standard deviation of 1.0 *mm/year*. The minimum and maximum differences were –1.5 *mm/year* and +2.2 *mm/year*, respectively. This result confirms the expected high accuracy achieved with the interferogram stacking technique. A more detailed description of this case was given by Strozzi et al., 1999.

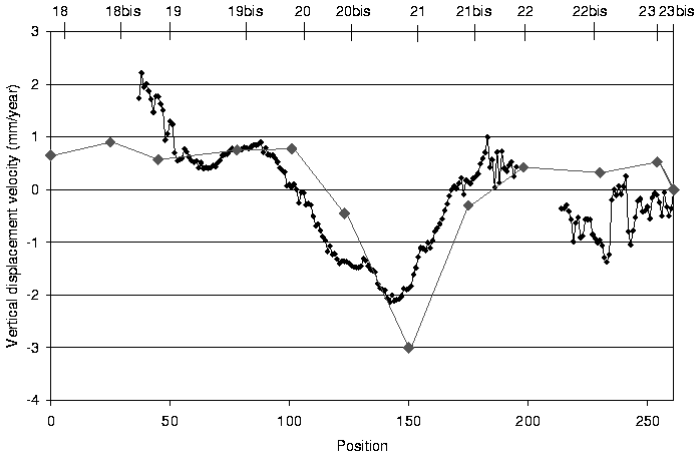

Figure 6. Profiles of the vertical displacement velocity from SAR interferometry (black line, period 1992-1996) and levelling surveys (gray line, period 1991-1995, data from Comune di Abano Terme and Regione del Veneto) along the levelling line Abano Terme – Montegrotto Terme (yellow line in Figure 5).

5. Conclusions

The feasibility of surface deformation mapping with ERS differential SAR interferometry was confirmed for a wide range of deformation velocities ranging from *m/year* (Ruhrgebiet, Mexico City) to *cm/year* (Bologna) and *mm/year* (Eugenean Geothermal Basin).

Data availability was found to be a limiting factor in the case of Mexico City. For the investigated European sites, on the other hand, a large number of ERS acquisition are available, allowing to optimize the data selection with respect to acquisition dates and interferometric baselines. For the planned future missions with SAR sensors which can be operated in a variety of modes

(ENVISAT, ALOS) this means that the robustness and operationality of the subsidence application relies very much on the selection of a single interferometric mode for most of the time.

As demonstrated for the Euganean Geothermal Basin the interferogram stacking technique allows to reduce the errors caused by atmospheric distortions to a low level making the measurement of slow deformation velocities in the *mm/year* range feasible. The technique also allows to increase the temporal resolution of the monitoring, as demonstrated with the annual monitoring of the subsidence for Bologna.

The main limitations of the interferometric technique are the temporal decorrelation of the signal, which leads to an incomplete coverage with deformation information, with gaps mainly in forested and agricultural areas, and the well known problems of the SAR imaging geometry in areas of rugged topography, such as layover and radar shadow.

The interferometric technique was found to be fast, as demonstrated by the fact that we are still waiting for the levelling data to validate the latest Bologna results, and cost effective.

Considering the high quality of the results achieved for the investigated sites, the huge SAR data archive starting in 1991, the expected continued availability of new SAR data, and the maturity of the required data processing techniques, we conclude that differential SAR interferometry has a very high potential for operational mapping of land subsidence.

The complementarity of the interferometric technique with levelling surveys and GPS measurements suggests that the most effective monitoring strategy will be an integration of the different techniques.

6. Acknowledgments

This work was supported by the ESA Data User Program (DUP). The Italian National Geologic Survey is acknowledged for the DEM.

7. References

Massonnet D., M. Rossi, C. Carmona, F. Adragna, G. Peltzer, K. Feigl, and T. Rabaute (1993), The displacement field of the Landers earthquake mapped by SAR interferometry, *Nature*, Vol. 364, No. 6433, pp. 138-142.

Massonnet, D., P. Briole, and A. Arnaud (1995) Deflation of Mount Etna monitored by spaceborne radar interferometry, *Nature*, Vol 375, pp. 567-570.

Goldstein R.M., R. Engelhardt, B. Kamb, and R. Frolich (1993), Satallite Radar Interferometry for Monitoring Ice Sheet Motion: Application to an Antarctic Ice Stream, *Science* Vol. 262, pp. 1525-1530, 3-dec-1993.

Strozzi T. and U. Wegmüller (1999a), Land Subsidence in Mexico City Mapped by ERS Differential SAR Interferometry, *Proc. IGARSS'99*, Hamburg, 28 June - 2 July.

Strozzi T., L. Tosi, L. Carbognin, U. Wegmüller, and A. Galgaro (1999b), Monitoring Land Subsidence in the Euganean Geothermal Basin with Differential SAR Interferometry, *Proc. Fringe'99*, Liège (B).

Strozzi T., U. Wegmüller, and G. Bitelli (2000), Differential SAR interferometry for land subsidence mapping in Bologna, *Proc. SISOLS'2000*, Ravenna, Italy, 25-29 September.

Wegmüller U. and T. Strozzi (1998a), Characterization of differential interferometry approaches, EUSAR'98, 25-27 May, Friedrichshafen, Germany, *VDE-Verlag, ISBN 3-8007-2359-X*, pp. 237-240.

Wegmüller U. and T. Strozzi, (1998b), SAR interferometric and differential interferometric processing chain. *Proc. of IGARSS'98*, Seattle, USA.

Wegmüller U. and T. Strozzi (1999), Validation of ERS Differential SAR Interferometry for Land Subsidence Mapping: the Bologna Case Study, *Proc. IGARSS'99*, Hamburg, 28 June - 2 July.